

Precision Neutrino Oscillation Measurements using Simultaneous High-Power, Low-Energy Project-X Beams

M.Bishai, M.Diwan, S.Kettell, J.Stewart, B.Viren, E.Worcester
Brookhaven National Laboratory

R.Tschirhart
Fermi National Accelerator Laboratory

L.Whitehead
University of Houston

Abstract

The first phase of the long-baseline neutrino experiment, LBNE10, will use a broadband, high-energy neutrino beam with a 10-kt liquid argon TPC at 1300 km to study neutrino oscillation. In this paper, we describe potential upgrades to LBNE10 that use Project X to produce high-intensity, low-energy neutrino beams. Simultaneous, high-power operation of 8- and 60-GeV beams with a 200-kt water Cerenkov detector would provide sensitivity to $\nu_\mu \rightarrow \nu_e$ oscillations at the second oscillation maximum. We find that with ten years of data, it would be possible to measure $\sin^2(2\theta_{13})$ with precision comparable to that expected from reactor antineutrino disappearance and to measure the value of the CP phase, δ_{CP} , with an uncertainty of $\pm(5 - 10)^\circ$. This document is submitted for inclusion in Snowmass 2013.

Recent measurements of non-zero $\sin^2(2\theta_{13})$ [1, 2, 3, 4] enable the search for CP violation in the neutrino sector and, ultimately, precision measurement of the CP phase, δ_{CP} , using $\nu_\mu \rightarrow \nu_e$ oscillations. The first phase of the long-baseline neutrino experiment, LBNE10, will use 708 kW of 120-GeV protons from Fermilab's Main Injector (MI) to produce a muon-neutrino or antineutrino beam aimed at a 10-kt liquid argon time projection chamber (LAr TPC) at a distance of 1300 km. The spectrum of neutrino energies detected at the far site in LBNE10 is aligned with the first oscillation maximum, peaking in the range

$E_\nu = (2-4)$ GeV. As described in its conceptual design report[5], LBNE10, in combination with other neutrino data, is expected to determine the neutrino mass hierarchy and provide an initial measurement of the CP phase in the three-generation framework.

Figure 1 shows the total neutrino-antineutrino asymmetry in the probability of $\nu_\mu \rightarrow \nu_e$ appearance as a function of δ_{CP} , at the first and second oscillation peaks, for normal and inverted hierarchy, at a distance of 1300 km. This asymmetry includes contributions from both CP and matter effects. It is clear from Fig. 1 that the matter effect is large in the first oscillation maximum, but in the second oscillation maximum, where $E_\nu = (0.2-1.5)$ GeV, the CP asymmetry is large with very little matter asymmetry. For this reason, measurement of $\nu_\mu \rightarrow \nu_e$ appearance at the second oscillation maximum provides excellent sensitivity to CP violation, independent of the mass hierarchy.

Project X[6] will make it possible to produce high-intensity, low-energy neutrino beams. In this paper, we summarize and update [7], which argues that simultaneous, high-power operation of 8- and 60-GeV beams with a 200-kt water Cerenkov detector at a long baseline provides sensitivity to $\nu_\mu \rightarrow \nu_e$ oscillations at the second oscillation maximum, allowing precise measurements of neutrino oscillation parameters independent of the mass hierarchy.

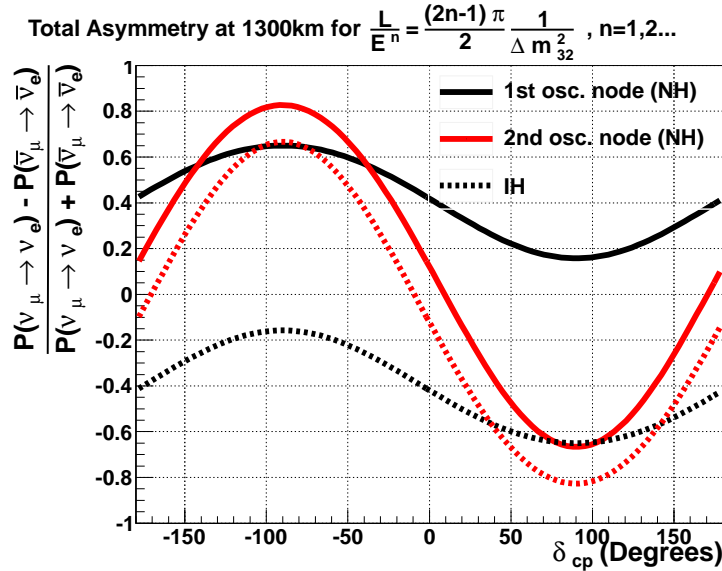


Figure 1: Total neutrino-antineutrino asymmetry in the probability of $\nu_\mu \rightarrow \nu_e$ appearance at 1300 km, at the first (black line) and second (red line) oscillation maxima, for normal (solid line) and inverted (dashed line) hierarchy, as a function of the true value of δ_{CP} .

The kinematics of neutrino beam production dictates that the only way to produce significant yield of neutrinos at low energies is with high proton-

Table 1: Summary of the oscillation parameters, constraints, and experimental assumptions that were used in the GLOBES calculations presented in this paper.

Parameter	Central Value	Uncertainty (1σ)
$\sin^2(\theta_{12})$	0.31	5%
θ_{23}	38.3°	8%
$\sin^2(2\theta_{13})$	0.094	5%
Δm_{21}^2	$+7.5 \times 10^{-5} \text{eV}^2$	3%
Δm_{31}^2 (NH)	$+2.5 \times 10^{-3} \text{eV}^2$	3%
Matter density	2.8 g/cm^3	2%
Signal normalization	n/a	1%
Background normalization	n/a	5%

beam power at low energies. With Project X, beam power from the MI can be maintained at or above 2 MW for proton energies of 60 GeV to 120 GeV. Upgrading to an 8-GeV pulsed LINAC would provide up to 4 MW of 8-GeV beam power, only 270 kW of which is required by the MI to produce the 2-MW, 60-GeV beam. In this scenario, the Fermilab accelerator complex could simultaneously produce 2 MW of 60-GeV protons and 3 MW of 8-GeV protons. The resulting neutrino beams would have significant flux with $E_\nu < 1.5$ GeV, which would allow measurement of $\nu_\mu \rightarrow \nu_e$ oscillation at the second oscillation maximum at 1300 km.

Here, we consider a 200-kt water Cherenkov detector, with reconstruction performance similar to Super-Kamiokande (SK)[8], located at Sanford Underground Research Facility (SURF)[9], as a potential future upgrade to LBNE. The efficiency of a water Cherenkov detector for quasielastic neutrino scattering, which dominates at low neutrino energy, is $\sim 80\%$. For this study, we have used GLOBES[10, 11] to estimate the experimental sensitivities using the oscillation parameters, constraints (where applicable), and experimental assumptions shown in Table 1. The central values of and constraints on the oscillation parameters are taken from a global fit to experimental neutrino data[12].

SK uses a log-likelihood (LL) variable to distinguish between ν_e charged-current signal and background. Log-likelihood variable cuts can be chosen such that there is 40% signal efficiency with little background or 80% signal efficiency with higher background levels. We have applied the SK 80% LL efficiencies for the 8-GeV beam, where background is expected to be low, and 40% LL efficiencies for the 60-GeV beam in which the background level is higher. Selection criteria could, of course, be optimized further, but we do not find large changes in the experimental sensitivity from tightening or loosening these cuts. Figure 2 shows the spectra for five years of neutrino and antineutrino running with the 8-GeV and 60-GeV beams, assuming normal hierarchy. The low-energy background level is significantly reduced relative to higher energy beams.

With ten years of running in simultaneous 8- and 60-GeV mode with a 200-kt water Cherenkov detector, in combination with data from LBNE10, it would be possible to measure both $\sin^2(2\theta_{13})$ and δ_{CP} very precisely. For the results

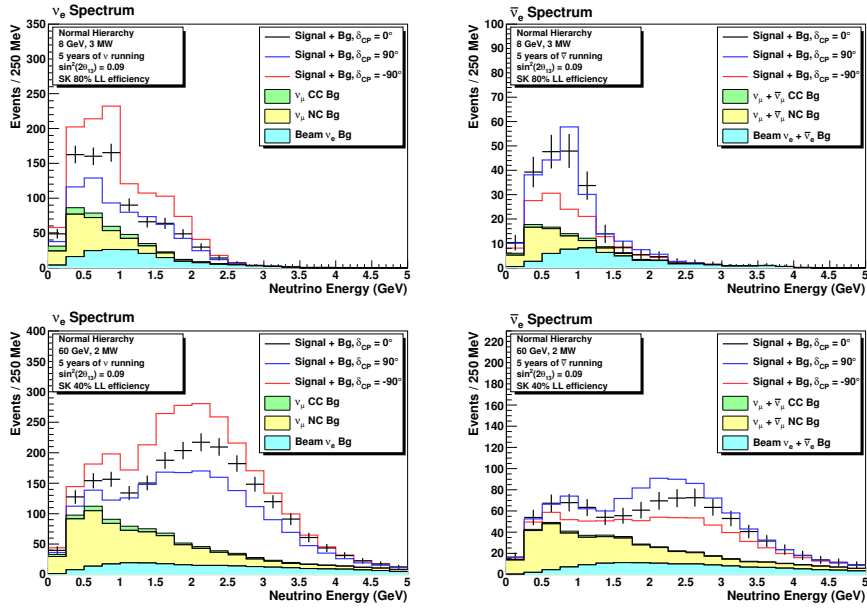


Figure 2: Expected signal and background distributions for neutrinos (left) and antineutrinos (right) for the 8-GeV (top) and 60-GeV (bottom) beams. The exposure is 5 years each for neutrinos and antineutrinos, with 3 MW of beam power for the 8-GeV beam and 2 MW of beam power for the 60-GeV beam. Normal hierarchy is assumed. The signal distributions for three possible values of δ_{CP} are shown. Efficiencies for the 8-GeV and 60-GeV data are calculated assuming SK 80% and 40% log-likelihood selection criteria, respectively.

shown here, we assume that the 8-GeV data is all in neutrino mode and the 60-GeV data is equally divided between neutrinos and antineutrinos. We do not include the contribution from additional data that could be taken with the LBNE10 LAr TPC during the ten years of low-energy running.

The 1σ contours from a two-dimensional fit to $\sin^2(2\theta_{13})$ and δ_{CP} for LBNE10, 60-GeV data, 8-GeV data, and the combination of the three are shown in Fig. 3. The precision on $\sin^2(2\theta_{13})$, coming primarily from the 120-GeV and 60-GeV data, is competitive with the precision expected from reactor neutrino experiments. The measurement of $\sin^2(2\theta_{13})$ is complementary to that from reactor neutrino experiments because it is measured in $\nu_\mu \rightarrow \nu_e$ oscillations rather than $\bar{\nu}_e \rightarrow \bar{\nu}_e$ disappearance. The 8-GeV and 60-GeV data are highly sensitive to δ_{CP} . The combination of 120-GeV, 60-GeV, and 8-GeV data provides a precise measurement of δ_{CP} with no external constraint on $\sin^2(2\theta_{13})$. Additionally, the 8-GeV, 60-GeV, and 120-GeV data place independent constraints on neutrino oscillation parameters; new physics could be detected as inconsistent measurements of neutrino oscillation parameters in these three data sets.

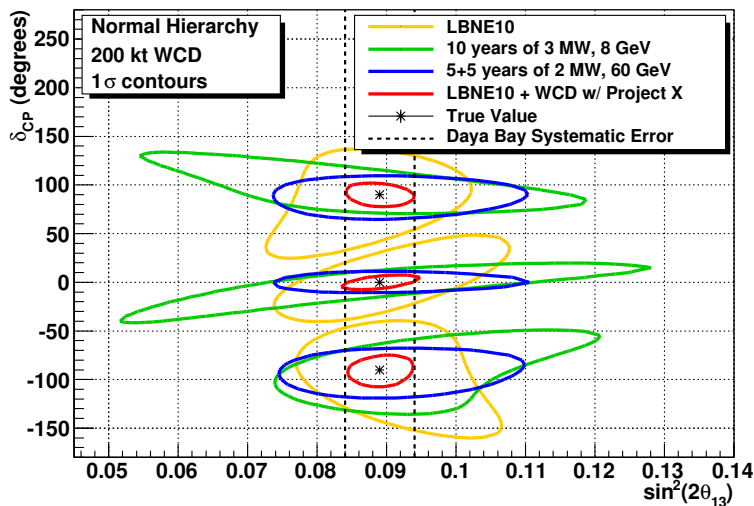


Figure 3: One-sigma contours from a two-dimensional fit for $\sin^2(2\theta_{13})$ and δ_{CP} for LBNE10(gold), 60-GeV data(blue), 8-GeV data(green), and the combination of the three(red). Fit results for three possible true values of δ_{CP} are shown. The Daya Bay systematic error on $\sin^2(2\theta_{13})$ (dashed lines) is shown for comparison.

Figure 4 compares the one-dimensional resolution on the measurement of δ_{CP} for simultaneous low-energy beams to LBNE LAr TPC detectors with a range of exposure to beams with energy 80-120 GeV, varying from 70 kt-MW-years to 750 kt-MW-years. Here we apply a 5% constraint on the value of $\sin^2(2\theta_{13})$ for all data sets. This constraint is consistent with the expected final

uncertainty on the value of $\sin^2(2\theta_{13})$ from reactor antineutrino disappearance experiments. This constraint is very important for the resolution of δ_{CP} at low exposures; for the simultaneous low-energy beams, such a constraint is less significant because the internal resolution on $\sin^2(2\theta_{13})$ is comparable to the external constraint. Ten years of data with a 200-kt WCD and simultaneous low-energy beams, in combination with LBNE10, provides the best δ_{CP} resolution for almost all true values of δ_{CP} , and is the only configuration considered that can reach 5° resolution for any value of δ_{CP} .

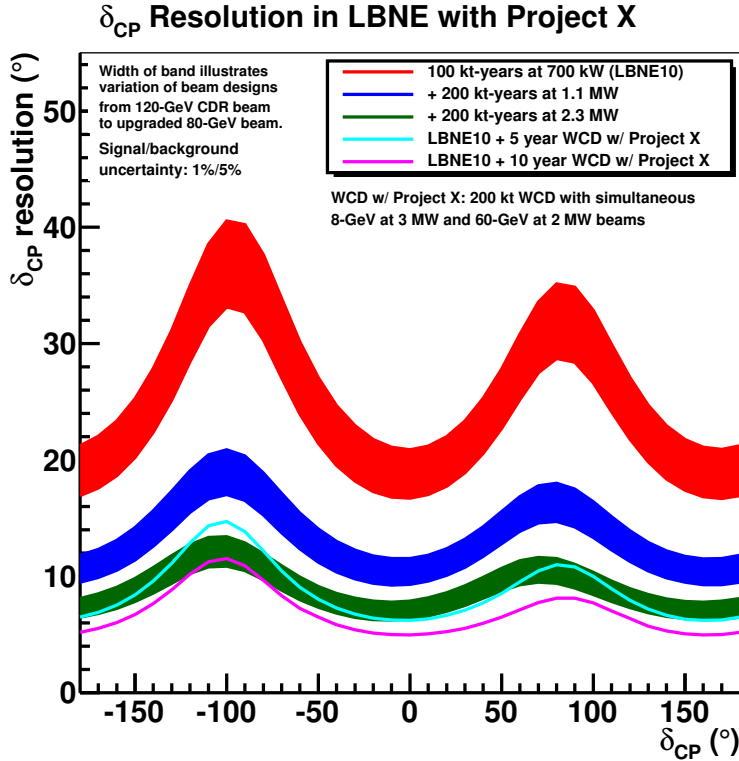


Figure 4: Resolution on the measurement of δ_{CP} as a function of the true value of δ_{CP} for various LBNE configurations. LBNE10 (red) refers to 100 kt-years of exposure to a 80-120 GeV, 700 kW beam for a LAr TPC. The blue and green curves show the resolution that can be achieved by a LAr TPC with higher exposures; total exposure for the blue curve is 290 kt-MW-years and for the green curve is 750 kt-MW-years. The cyan and pink curves show the resolution for LBNE10 in combination with five and ten years, respectively, of simultaneous, low-energy beams and a 200-kt WCD, as described in this paper.

Adding the 8- and 60-GeV data to LBNE10 also significantly improves sensitivity to resolution of the θ_{23} octant degeneracy. Figure 5 shows the signifi-

cance of the octant determination for LBNE10, 60-GeV data, 8-GeV data, and the combination of the three, as a function of the true value of θ_{23} . In this fit, $\nu_\mu \rightarrow \nu_\mu$ disappearance contributes to the precision on $\sin^2(2\theta_{23})$ while the $\nu_\mu \rightarrow \nu_e$ appearance data provides information on the θ_{23} octant. Again, a 5% external constraint on the true value of $\sin^2(2\theta_{13})$ has been applied; this is necessary for the LBNE10 analysis, but becomes less important with the addition of the low-energy data. A 5σ determination of the octant of θ_{23} will be possible for at least 90% of true values of δ_{CP} for $41^\circ < \theta_{23true} < 51^\circ$. Most of the sensitivity comes from the 120-GeV and 60-GeV data because the second oscillation maximum does not provide any special sensitivity to the octant determination.

Octant Sensitivity

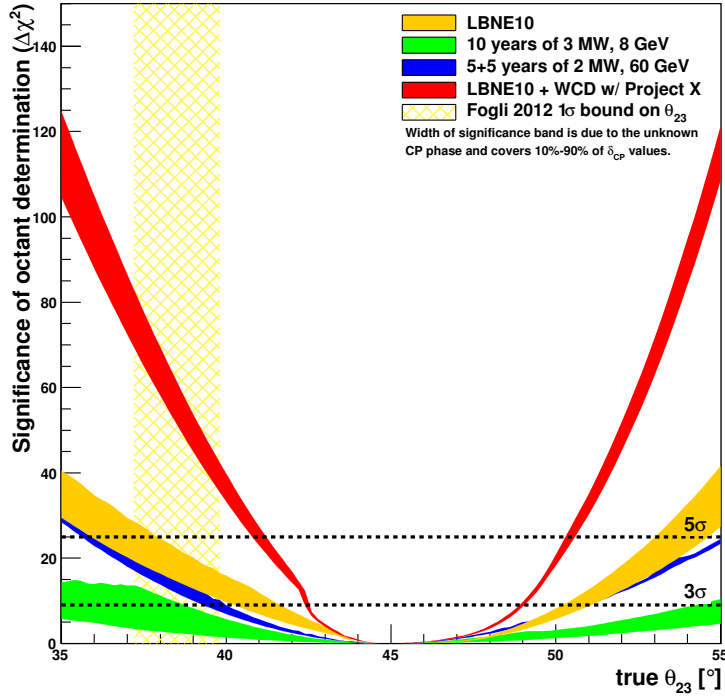


Figure 5: Significance of the octant determination ($\Delta\chi^2$ for a fit to the “wrong” octant) as a function of the true value of θ_{23} for LBNE10(gold), 60-GeV data(blue), 8-GeV data(green), and the combination of the three(red). The width of each curve is due to the unknown CP phase and covers 10% to 90% of possible true δ_{CP} values. The 1σ bound on θ_{23} from a global fit to neutrino experimental data[12] is shown in yellow for reference.

In summary, the cleanest, most dramatic sensitivity to the CP phase comes from measurement of $\nu_\mu \rightarrow \nu_e$ oscillation at the second oscillation maximum,

at long baseline, with a high-mass far detector. Project X, with an 8-GeV pulsed LINAC, could produce simultaneous low-energy, high-intensity beams which probe this low-energy region, making precision measurements of neutrino oscillation parameters possible.

References

- [1] F. An *et al.*, “Observation of electron-antineutrino disappearance at Daya Bay,” *Phys. Rev. Lett.*, vol. 108, p. 171803, 2012, arXiv:1203.1669.
- [2] J. Ahn *et al.*, “Observation of reactor antineutrino disappearance in the RENO experiment,” *Phys. Rev. Lett.*, vol. 108, p. 191802, 2012, arXiv:1204.0626.
- [3] Y. Abe *et al.*, “Reactor electron antineutrino disappearance in the Double Chooz experiment,” *Phys. Rev. D*, vol. 86, p. 052008, 2012, arXiv:1207.6632.
- [4] F. An *et al.*, “Improved measurement of electron antineutrino disappearance at Daya Bay,” *Chinese Physics C*, vol. 37, p. 011001, 2013, arXiv:1210.6327.
- [5] “Long-Baseline Neutrino Experiment (LBNE) Project: Conceptual Design Report,” 2012. <http://lbne.fnal.gov/papers.shtml>.
- [6] “Project X: Accelerator Overview,” 2012. <http://projectx.fnal.gov/pdfs/ProjectX-accelerator-overview.pdf>.
- [7] M. Bishai *et al.*, “Neutrino oscillations in the precision era,” 2012, arXiv:1203.4090.
- [8] “Atmospheric neutrino oscillation analysis with subleading effects in Super-Kamiokande I, II, and III,” *Phys. Rev. D*, vol. 81, p. 092004, 2010.
- [9] <http://sanfordlab.org>.
- [10] P. Huber, M. Lindner, and W. Winter, “Simulation of long-baseline neutrino oscillation experiments with GLOBES (General Long Baseline Experiment Simulator),” *Comput.Phys.Commun.*, vol. 167, p. 195, 2005, hep-ph/0407333.
- [11] P. Huber, J. Kopp, M. Lindner, M. Rolinec, and W. Winter, “New features in the simulation of neutrino oscillation experiments with GLOBES 3.0: General Long Baseline Experiment Simulator,” *Comput.Phys.Commun.*, vol. 177, pp. 432–438, 2007, hep-ph/0701187.
- [12] G. Fogli *et al.*, “Global analysis of neutrino masses, mixings and phases: entering the era of leptonic CP violation searches,” 2012, arXiv:1205.5254.